J. Biochem. **128**, 481–491 (2000)

Common Architecture of the Primary Galactose Binding Sites of *Erythrina corallodendron* Lectin and Heat-Labile Enterotoxin from *Escherichia coli* in Relation to the Binding of Branched Neolactohexaosylceramide[1]

Susann Teneberg, Anna Berntsson, and Jonas Ångström[2]

Institute of Medical Biochemistry, Göteborg University, P.O. Box 440, SE 405 30 Göteborg, Sweden

Received May 18, 2000; accepted June 23, 2000

The heat-labile enterotoxin from *Escherichia coli* (LT) is responsible for so-called traveller's diarrhea and is closely related to the cholera toxin (CT). Toxin binding to GM1 at the epithelial cell surface of the small intestine initiates the subsequent diarrheal disease. However, LT has a broader receptor specificity than CT in that it also binds to *N*-acetyllactosamine–terminated structures. The unrelated lectin from *Erythrina corallodendron* (ECorL) shares this latter binding property. The findings that both ECorL and porcine LT (pLT) bind to lactose as well as to neolactotetraosylceramide suggests a common structural theme in their respective primary binding sites. Superimposing the terminal galactose of the lactoses in the respective crystal structures of pLT and ECorL reveals striking structural similarities around the galactose despite the lack of sequence and folding homology, whereas the interactions of the penultimate GlcNAcβ3 in the neolactotetraosylceramide differ. The binding of branched neolactohexaosylceramide to either protein reveals an enhanced affinity relative to neolactotetraosylceramide. The β3-linked branch is found to bind to the primary Gal binding pocket of both proteins, whereas the β6-linked branch outside this site provides additional interactions in accordance with the higher binding affinities found for this compound. While the remarkable architectural similarities of the primary galactose binding sites of pLT and ECorL point to a convergent evolution of these subsites, the distinguishing structural features determining the overall carbohydrate specificities are located in extended binding site regions. In pLT, Arg13 is thus found to play a crucial role in enhancing the affinity not only for *N*-acetyllactosamine–terminated structures but also for GM1 as compared to human LT (hLT) and CT. The physiological relevance of the binding of *N*-acetyllactosamine–containing glycoconjugates to LT and ECorL is briefly discussed.

Key words: binding site structural motifs, docking studies, *Erythrina corallodendron* lectin, *Escherichia coli* heat-labile enterotoxin, *N*-acetyllactosamine binding.

Although the two proteins under investigation in the present paper, the dimeric lectin (ECorL) from seeds of the *Erythrina corallodendron* tree (*1*) and the heat-labile heterohexameric AB_5 toxin (LT) from *Escherichia coli* (*2*), have quite different origins, they have been found to share a common binding specificity in that both bind to the *N*-acetyllactosamine–terminated structure neolactotetraosylceramide (*3*, *4*) as well as to galactose and lactose (*5–8*). For ECorL, whose biological function is unknown, we recently showed that this lectin actually should be considered fucosyl-*N*-acetyllactosamine–specific rather than just *N*-acetyllactosamine–specific (*9*) due to the excellent fit of Fucα2 into an extended binding pocket providing additional interactions that explain the enhanced affinity of the H5 type 2 glycosphingolipid relative to neolactotetraosylceramide. Regarding LT, other receptors in addition to the natural GM1 receptor [Galβ3GalNAcβ4(NeuAcα3)Galβ4Glcβ1Cer] have been proposed to explain the fact that the physiological effects of this toxin, in contrast to cholera toxin (CT) from *Vibrio cholerae*, cannot be completely inhibited by the addition of CT B-pentamers that block access to GM1 for both toxins. Neolactotetraosylceramide or similarly terminated compounds of glycosphingolipid origin (*4*, *10*) thus represent potential receptor candidates, as do glycoproteins from different sources containing terminal Galβ4GlcNAcβ3 sequences that may or may not be branched (*11–16*).

In this context the present finding that LTs [especially LT of porcine origin (pLT)], but not CT, bind significantly to the branched model compound neolactohexaosylceramide [Galβ4GlcNAcβ6(Galβ4GlcNAcβ3)Galβ4Glcβ1Cer] is relevant for the observed broader range of specificities of this

[1] This work was supported by grants from the Swedish Medical Research Council (Nos. 3967, 10435, and 12628), the Cancer Foundation and the Wallenberg Foundation.

[2] To whom correspondence should be addressed. Phone: +46-31-7733049, Fax: +46-31-413190, E-mail: Jonas.Angstrom@medkem.gu.se

Abbreviations: ECorL and rECorL, native and recombinant forms of the *Erythrina corallodendron* lectin, respectively; LT, *Escherichia coli* heat-labile enterotoxins, pLT and hLT, heat-labile enterotoxins originating from porcine and human *Escherichia coli* strains, respectively; CT, cholera toxin; LTB, pLTB, hLTB, and CTB, B-pentamers of each respective toxin; r.m.s., root mean square.

toxin. Furthermore, since ECorL is also capable of binding branched neolactohexaosylceramide, it was considered of prime importance to elucidate the structural rationales behind the observed common binding specificities of these two proteins. Moreover, from the crystal structures of ECorL (*5*, *6*) and pLT (*7*), both in complex with lactose, it has been pointed out that pLT shares with other lectins, among them ECorL, the structural trait of having an aromatic residue closely stacked onto the terminal Galβ4 residue of lactose, thus providing a hydrophobic interface that contributes significantly to the binding affinity of this ligand (*17*).

In the present paper, we use molecular modeling to show that the structural similarities in the primary galactose site of the respective binding pockets go far beyond this single instance and that, furthermore, binding to *N*-acetyllactosamine–terminated structures, linear or branched, occurs despite the lack of sequence and folding homology between the two proteins. The enhanced affinities of both proteins for branched neolactohexaosylceramide relative to neolactotetraosylceramide, as found using the microtiter well assay, is thus shown in both cases to result from additional interactions provided by the β6-linked branch in extended but very different binding sites. The major driving force for binding is, however, provided by the β3-linked branch in the primary galactose binding site in each case. These findings were corroborated by the binding of branched neolactohexaosylceramide to either naturally occurring or genetically engineered variants of the two proteins.

MATERIALS AND METHODS

Glycosphingolipids—The glycosphingolipids used in the present study were isolated as described earlier (*18*), and the identity of the purified compounds was established by mass spectrometry, ^{1}H NMR spectroscopy and degradation studies, as outlined in Ref. *3*. Lactosylceramide (Galβ4-Glcβ1Cer) was obtained from dog small intestine (*19*), neolactotetraosylceramide (Galβ4GlcNAcβ3Galβ4Glcβ1Cer) from human erythrocytes (*20*), the branched structures Galβ4GlcNAcβ6(Galβ4GlcNAcβ3)Galβ4Glcβ1Cer and Galβ4GlcNAcβ6(NeuAcα3Galβ4GlcNAcβ3)Galβ4Glcβ1Cer from bovine buttermilk (*3*), and GM1 [Galβ3GalNAcβ4(NeuAcα3)Galβ4Glcβ1Cer] from human brain (*21*). The linear structure Galβ4GlcNAcβ3Galβ4GlcNAcβ3Galβ4Glcβ1Cer was obtained by mild acid hydrolysis of the corresponding sialic acid–terminated compound isolated from rabbit thymus (*22*).

Lectins and Toxins–Native ECorL was purchased from Sigma; rECorL and the Trp135Tyr mutant were prepared as described (*23*). The recombinant form differs from the native protein at seven positions in the sequence as follows: Asp23Ala, Ser24Ala, Pro26Ile, Glu27Thr, Thr28Gln, Phe113Asn, and Pro134Gln (*24*). However, only the last alteration is sufficiently close to the saccharide binding site region to have any bearing on the results presented below. Pentameric B-subunits from CT were obtained from List Biological Laboratories, Campbell, CA, while pLTB and hLTB (derived from porcine *E. coli* strain P307 and human *E. coli* strain H74-114, respectively) were prepared as described (*25*). Protein labeling with ^{125}I was performed by the Iodogen method (*26*).

The binding of radiolabeled lectins or toxin B pentamers to glycosphingolipids adsorbed in microtiter wells was done as described (*3*, *4*, *27*). Briefly, serial dilutions (each in triplicate) of pure glycosphingolipids in methanol were applied to microtiter wells (Falcon 3911, Becton Dickinson Labware, Oxnard, CA), and kept at room temperature (RT) until the solvent had evaporated. To diminish unspecific protein binding, the wells were coated with 200 μl of phosphate-buffered saline (PBS), pH 7.3, containing 2% (w/v) bovine serum albumin, and 0.1% (w/v) NaN_3 (Sol. I) for 2 h at RT. After washing once with Sol. I, radiolabeled lectins or toxin B pentamers were added to the wells (50 μl/well; diluted to approximately 2×10^3 or 5×10^3 cpm/μl, respectively, in Sol. I), and the plates were incubated for 4 h at RT. The wells were then washed six times with Sol. I, and, after drying, the radioactivity was counted in a gamma counter.

For inhibition studies, 10 μg of ^{125}I-labeled hLTB in 100 μl Sol. I (4×10^3 cpm/μl) was incubated with 10 mM GM1 pentasaccharide (Alexis Corp., San Diego, CA) or 10 mM neolactotetraose (IsoSep, Tullinge, Sweden) for 2 h at RT. Thereafter, the suspensions were diluted 40 times (giving 1×10^3 cpm/μl), and utilized in the microtiter well assay, as detailed above.

Molecular Modeling—Molecular modeling was conducted on a Silicon Graphics Indigo^{2}Extreme workstation using the Quanta97/CHARMm22 software package (Molecular Simulations) or on a Silicon Graphics 4D/35TG workstation using the Biograf software package (Molecular Simulations). Protein models were constructed based on the crystal structures of the complex between ECorL and lactose (*5*, *6*) and that of pLT and lactose (*7*), both structures available at the Brookhaven Protein Data Bank (entries 1LTE, 1AX1, and 1LTT, respectively). Solvent molecules were removed, except those that were completely surrounded by the protein environment. The *N*-linked heptasaccharide of ECorL (at Asn-17) was also removed since it is far from the binding site. Subsequently, both polar and nonpolar hydrogens were added to the structures. For pLT, a partial structure consisting of one whole B subunit (H) and a loop (residues 25–40) from one of the neighboring subunits (D) was used in docking and dynamics simulations. To refine the stereochemistry and molecular contacts, constrained energy minimizations of the proteins were carried out. Harmonic constraints of 20 kcal/mol/Å^2 were applied to all α carbons, and, in the case of ECorL, also the two metal ions present in the lectin (Ca^{2+} and Mn^{2+}), as well as to the oxygen atoms of the internal water molecules, during 100 steps of steep descent geometry relaxation. Afterwards, harmonic constraints were reduced to 5 kcal/mol/Å^2 in order to perform 300 steps of conjugate gradient minimization. A distance dependent dielectric constant ($\varepsilon = 6r$) and a 15 Å cutoff distance were used for nonbonded interactions. For ECorL, the r.m.s. deviation from the crystal structure at the end of this procedure was 0.10 Å when calculated for main chain atoms and 0.41 Å for all atoms in the protein. The Ca^{2+} and Mn^{2+} ions were displaced from their crystal positions by 0.05 and 0.15 Å, respectively. For pLT, the r.m.s. deviations from the crystal structure were 0.22 and 0.47 Å for the main chain atoms and the whole substructure, respectively. These structures were subsequently used as starting geometries in the docking procedures.

Generation of Ligand Conformations and Docking—A previous examination of the glycosidic angles of an *N*-ace-

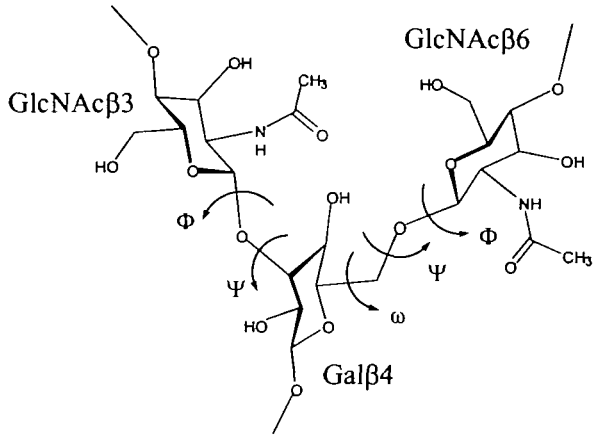

Fig. 1. **Schematic structure of the branched trisaccharide fragment [GlcNAcβ6(GlcNAcβ3)Galβ4] of neolactohexaosylceramide showing linkages and glycosidic dihedral angles.** The glycosidic dihedral angles are defined as Φ = H-1–C-1–O-1–C-6, Ψ = C-1–O-1–C-6–C-5, and ω = O-1–C-6–C-5–O-5 for 6-linked residues, whereas angles are defined as Φ = H-1–C-1–O-1–C-X and Ψ = C-1–O-1–C-X–H-X for other linkages (X = 2, 3, or 4).

tyllactosamine–based biantennary octasaccharide with a mannose core in complex with the lectin (LOL1) from *Lathyrus ochrus* (*28*), and the glycosidic angles of the constituent disaccharides, as found by molecular modeling, revealed that, for all but one of the linkages in the complex, minima other than the global ones were occupied (*29*). Since an analogous situation could not be excluded in the case of neolactohexaosylceramide complexed to pLT or ECorL, attempts to explore the energy surface of the isolated oligosaccharide were restricted to the trisaccharide at the branching point. Different conformers of the oligosaccharide part of neolactohexaosylceramide were thus generated for docking and dynamics studies by examining the possible energy minima of the GlcNAcβ6(GlcNAcβ3)Galβ4 fragment. The GlcNAcβ6Galβ4 glycosidic dihedral angles (Φ, Ψ as defined in Fig. 1) were allowed to vary for fixed values of the ω dihedral angle, corresponding to the three staggered orientations of the C5-C6 bond of Galβ4, while keeping the GlcNAcβ3Galβ4 glycosidic angles (31°, 29°) constant (*29*). Once the various minima were located, the terminal galactoses and the glucose at the reducing end were added using literature values for their glycosidic angles (*29*, *30*), and then energy minimization (ε = 3.5r) of each conformer was performed (Table I). These conformers were subsequently used as starting structures for molecular dynamics runs on the isolated oligosaccharide. Docking was performed by superimposing the terminal galactose ring of either the β3- or the β6-linked branch of the oligosaccharide part of neolactohexaosylceramide onto the terminal galactose of lactose in either ECorL or pLT. In these generated complexes, the minimum energy conformation of the superimposed Galβ4GlcNAc segment was chosen so that the penultimate GlcNAc residue overlapped the same residue of the *N*-acetyllactosamine complex of ECorL (*6*, *9*) and the neolactotetraose complex of pLT (*4*). This appears justified when comparing, *e.g.*, complexes of LOL1 with the biantennary octasaccharide mentioned above (*28*) and the Manα3Manβ4GlcNAc trisaccharide (*31*). A comparison thus shows that the Manα3Man segments virtually overlap

TABLE I. **Minimum energy conformations of branched neolactohexaosylceramide for varying glycosidic dihedral angles of the GlcNAcβ6Gal segment.**

Conformer	Φ/Ψ/ω[a] (degrees)	Relative energy (kcal/mol)	Comment
1	45/–111/–58	8.6	Extended
2	35/–105/71	2.9[b]	Backfolded
3	–30/178/64	6.0	T-shaped
4	177–158/–52	3.1	T-shaped
5	45/–100/–176	0.4	T-shaped
6	52/142/175	0.1	Extended
7	44/74/42	0.0[b]	Backfolded

[a]See legend to Fig. 1 for a definition of the glycosidic dihedral angles. [b]The β6-linked branch interacts with the ceramide in these two cases, resulting in energies that are too favorable when compared with other conformers. In addition, conformers 2 and 7 would probably not be allowed with the glycosphingolipid inserted into a membrane bilayer. Thus, conformer 6 most likely represents the energetically most favored conformation.

despite the very different natures of the two ligands. Hydroxyl groups in both the protein and ligand were oriented so as to favor hydrogen bond interactions. Finally, energy minimizations were carried out for each complex using the dielectric constants chosen for subsequent molecular dynamics simulations.

Molecular Dynamics Simulations—Dynamics simulations were run in a vacuum and/or in a water environment. A distance-dependent dielectric constant ε = 6r (CHARMm) or ε = 3.5r (Dreiding), and a constant one (ε = 1) were used for vacuum and water simulations, respectively. The SHAKE algorithm as implemented in CHARMm was used to constrain bonds containing hydrogen atoms, allowing a time step of 0.002 ps in vacuum and 0.001 in the presence of explicit water molecules. Simulations (CHARMm) were started by heating the system from 0 K to the final temperature (300 K) in 5 K increments every 100 time steps, followed by an equilibration period of 10 ps. Simulations (Dreiding) on isolated oligosaccharides were performed with a time step of 0.001 ps using the Nosé-Hoover algorithm at 300 K (*32*).

RESULTS AND DISCUSSION

Binding of N-Acetyllactosamine–Terminated Glycosphingolipids—In Fig. 2 the results of the binding of pLTB (A) and ECorL (B) to different glycosphingolipids immobilized in microtiter wells are shown. A comparison of the estimated binding affinities for neolactotetraosylceramide (Galβ4GlcNAcβ3Galβ4Glcβ1Cer) and branched neolactohexaosylceramide [Galβ4GlcNAcβ6(Galβ4GlcNAcβ3)Galβ4Glcβ1Cer] reveals that the lectin binds the latter compound approximately three times more strongly than neolactotetraosylceramide, whereas the toxin binds the branched neolactohexaosylceramide with approximately five times higher affinity. However, relative to the natural receptor, GM1 ganglioside, the toxin affinity for both *N*-acetyllactosamine–containing glycosphingolipids is low (*cf.* Fig. 7). The extension of neolactohexaosylceramide by an α6-linked sialic acid on the β3-linked arm results in both proteins being unable to bind to this compound. It should be pointed out that both proteins bind to lactose, as evidenced by the published crystal structures (*5*, *7*). Lactosylceramide is, however, non-binding in the microtiter well assay in the

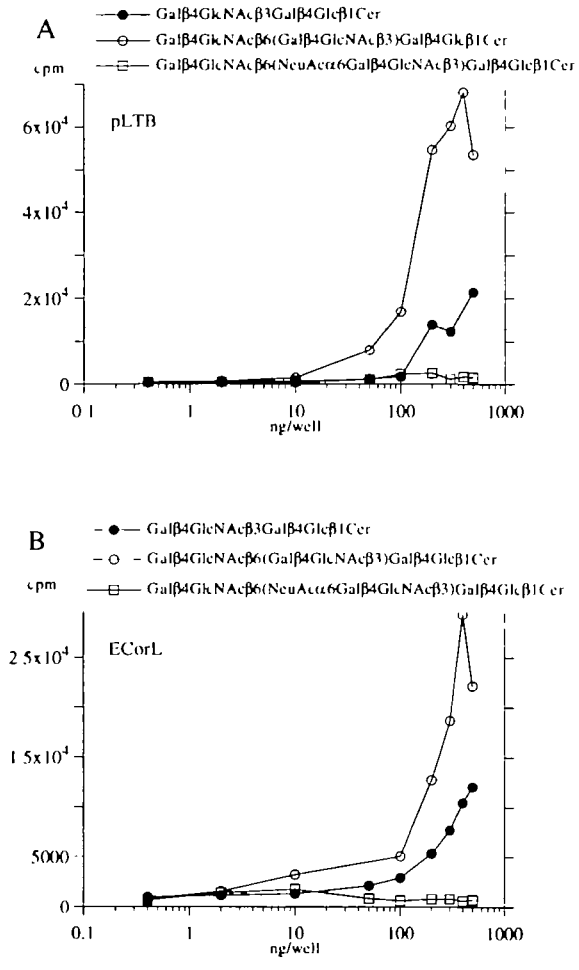

Fig. 2. **Microtiter well assay results for the binding of B-subunits from porcine heat-labile enterotoxin (pLTB) from *Escherichia coli* (A) and lectin (ECorL) from *Erythrina corallodendron* (B) to *N*-acetyllactosamine-containing glycosphingolipids.** The proteins were ^{125}I-labeled and added to serial dilutions of glycosphingolipids adsorbed in microtiter wells. The data represent mean values of triplicate determinations.

case of ECorL (*3*), and LT isolated from an *E. coli* strain of human origin (*33*), most likely due to the relatively low sensitivity of this assay system.

Primary Galactose Site Architecture—The findings that both pLT and ECorL bind lactose and neolactotetraosylceramide as well as the branched version of neolactohexaosylceramide is strongly suggestive of a common structural theme in the binding site topology of the two proteins, especially with regard to the primary galactose binding pockets, which provide most of the energetic driving force in the binding process for lactose. The availability of the crystal structures of pLT (*7*) and ECorL (*5*, *6*) in complex with lactose allows a close scrutiny of the above supposition. Figure 3 thus shows these two structures superimposed so that the terminal Galβ4 units of the lactose overlap completely, and the interactions of the sugar moiety with each respective protein are summarized in Table II.

It is clear that the overall topologies of these two structures bear no resemblance to each other, as would be expected from the lack of sequence homology between the proteins. Inspection of Fig. 3 and Table II reveals, however, that hydrogen bond interactions around the perimeter of the galactose in one of the complexes are afforded by the same or conservatively replaced amino acid side chains in several instances in the other, and, as pointed out (*17*), that stacking an aromatic residue, Trp88 in pLT and Phe131 in ECorL, against the hydrophobic face of the galactose is evident in both complexes. Residues Glu51, Gln56, Gln61, Trp88, and Asn90 in pLT are thus echoed by residues Asp89, Ala218, Gln219, Phe131, and Asn133, respectively, in ECorL. In the case of the Gln56–Ala218 pair it is the β,γ-methylene segment of the former residue that mimics the role of the methyl group of the latter residue. Due to the different folding patterns, some of the amino acid side chains approach the galactose from somewhat different directions as exemplified by the Asn133 side chain in ECorL, which is located ~2.8 Å behind Asn90 in pLT (Fig. 3) allowing hydrogen bonding with only the Galβ4 3-OH in the former case. A similar example is given by the Asp89 side chain in ECorL, which is situated ~2.6 Å to the left relative to Glu51 in pLT, yielding, in the case of ECorL, only one hydrogen bond with the Galβ4 4-OH. A third example stems from the location of the Gln219 side chain in ECorL, which, compared to Gln61 in pLT, is found ~3.4 Å below and in front of the former residue. Both complexes also exhibit two bridging water molecules in roughly similar locations, providing additional hydrogen bond interactions for the 2-OH and 6-OH of the galactose, whereas a third water molecule in pLT, partly interacting with 6-OH, is compensated for by hydrophobic interactions between Ala88 β-CH_3 and Galβ4 6-CH_2 in ECorL. Lastly, an important feature in both complexes is represented by the partial closure of the galactose binding pocket by, in the case of EcorL, the methyl group of Ala218 and, in the case of pLT, the β,γ-methylene segment of Gln56.

Considering the diverse origins of these two proteins, the nearly identical structural features around the primary galactose binding sites in ECorL and pLT represent an example of convergent evolution that is quite striking. Oligosaccharide specificity is thus conferred by sugar units outside the anchor position taken up by the terminal galactose as manifested by the crystal structure of the CTB-GM1 pentasaccharide complex (*34*) and the structure of the terminal trisaccharide of the H5 type 2 glycosphingolipid in complex with ECorL obtained by molecular modeling (*9*).

Docking of Branched Neolactohexaose—Despite the fact that the optimal receptor structures for pLT and ECorL differ significantly from each other, it is evident that these two proteins, apart from lactose binding, share further binding characteristics in that they both bind to linear (*3*, *4*, *10*) and branched *N*-acetyllactosamine-containing glycosphingolipids (Fig. 2). The additional interactions provided by the penultimate GlcNAcβ3 residue of neolactotetraosylceramide has been described (*4*, *9*) and found to differ in the two complexes. Whereas the enhanced affinity, relative to lactose, in ECorL is provided by hydrogen bond interactions between the Gln219 side chain and the acetamido and 3-OH groups of GlcNAcβ3 [see also the recent crystal structure of the *N*-acetyllactosamine–ECorL complex by Elgavish and Shaanan (*6*)], corresponding interactions for pLT are found on the opposite side of this sugar residue involving hydrogen bond interactions between the 6-OH and the Arg13 side chain.

Further enhancement of the affinity of both ECorL and

TABLE II. **Comparison of interactions of the terminal galactose of lactose in complex with pLT and ECorL.**

Galactose	Interacting protein moiety and water		Type of interaction	Comment
	pLT	ECorL		
2-OH	Asn90 δ2-NH (2.9)		Hydrogen bond	
2-OH	Water (3.0)	Water (3.8)	Hydrogen bond	Bridge to Arg13 CO and Asn133 δ2-NH, resp.
3-OH	Asn90 δ1-O (2.8)	Asn133 δ2-NH (3.1)	Hydrogen bond	
	Lys91 ξ-NH_3 (3.0)	Gly107 NH (2.9)	Hydrogen bond	
		Asp89 δ2-O (2.8)	Hydrogen bond	
4-OH	Glu51 ε1-O (3.3)	Asp89 δ1-O (2.8)	Hydrogen bond	
	Lys91 ξ-NH_3 (2.8)	Ala218 NH (2.9)	Hydrogen bond	
6-OH	Gln61 ε2-NH (2.9)	Gln219 ε2-NH (3.2)	Hydrogen bond	
	Water (2.9)	Water (2.9)	Hydrogen bond	Bridge to Gly33 NH and Leu86 CO, resp.
	Water (3.8)		Hydrogen bond	Bridge to Gln56 CO
3-H, 4-H, 5-H	Trp88 indole	Phe131 phenyl	Hydrophobic	
4-H, 6-H		Ala88 β-CH_3	Hydrophobic	
6-CH_2OH	His57 δ2-CH, ε2-NH	Ala222 β-CH_3	Steric	
Hydrophilic face	Gln56 β,γ-CH_2	Ala218 β-CH_3	Steric	Closing of binding site
Hydrophilic face	Lys91 ξ-NH_3	Tyr106 β-CH_2	Steric	Closing of binding site

*Data are taken from the crystal structures of pLT (7) and ECorL (5). Figures given in parentheses are rounded values for distances (Å) between the hydrogen bond donor and acceptor atoms. It should be noted that in the more recently determined crystal structure of ECorL-lactose complex (6), an additional water molecule was found bridging the Gly107 NH and the Gal 3-OH groups. No corresponding interaction is found for the pLT-lactose complex.

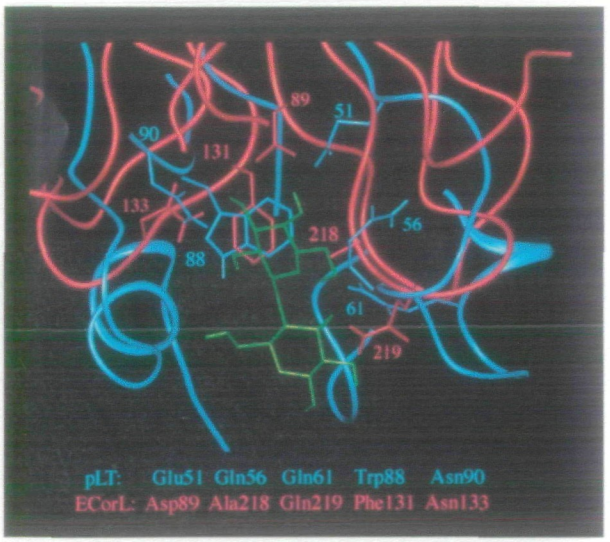

Fig. 3. **Comparison of the binding site regions of the lactose complexes of the lectin from *Erythrina corallodendron* (ECorL) and the heat-labile toxin from *Escherichia coli* (pLT).** Alignment of the two complexes was achieved by superimposing the terminal galactose of the bound lactose in one complex onto the same sugar residue in the other. The ECorL backbone and selected amino acid side chains are shown in red while the corresponding features for pLT are in blue and the lactose (originating from the pLT complex) is in green. Protons bonded directly to carbon atoms are not included. Important interactions between the galactose of lactose and the respective protein are given in Table II.

pLT is obtained by the addition of a β6-linked *N*-acetyllactosamine branch to the internal galactose of neolactotetraosylceramide as shown in Fig. 2, suggesting additional interactions provided by this extension. In principal, both the β3- and β6-linked branches are capable of binding to the respective binding sites of the proteins, but the docking of the latter branch, using different minimum energy conformers as listed in Table I, results in either severe clashes of the former branch with protein moieties or no interaction at all in the case of pLT. Furthermore, in some cases, unlikely conformations around the Glcβ1Cer linkage would have to be adopted in order to present the binding epitope properly. However, for ECorL, either branch may dock into the galactose site without the other interfering sterically with the protein as will be shown below. The fact that sialylation of the β3-linked branch causes a complete loss of binding of either protein (Fig. 2) may be rationalized by findings from a 1 ns dynamics simulation of the isolated oligosaccharide, which show that, for extended conformations, the sialic acid interferes substantially with the β6-linked branch, but most of the time T-shaped or backfolded conformations are present. None of these conformations is compatible with binding of the β6-linked branch into the primary Gal site.

Docking of the β3-linked branch of the oligosaccharide part of neolactohexaosylceramide into the ECorL binding site reveals that only extended conformations (conformers 1 and 6 in Table I) provide additional interactions with the protein. The difference between these two conformers consists of an approximately 180° turn of the β6-linked branch around the long axis of the disaccharide unit with conformer 6 being the energetically favored species. Dynamics simulations on the isolated oligosaccharide using different starting conformations according to Table I reveal that conformer 6 is completely dominating when starting from either conformer 5 or 6 (not shown), whereas conformer 1 as the starting conformation gives rise mainly to T-shaped or backfolded conformers. Transitions to conformers 5 and 6 were not observed. Nevertheless, the complex between ECorL and conformer 1 was investigated by a 100 ps dynamics simulation in which the terminal galactose of the β3-linked branch was found to have lost several of the important interactions in the primary galactose site (described above) due to a 3–4 Å downward twisting movement initiated by attempts of the β6-linked branch to attain more energetically favorable conformations. Towards the end of the simulation, the whole oligosaccharide had assumed a position in which the glucose end had rotated approximately 60° towards the viewer relative to the view shown in Fig. 4 (see below). It is thus clear that this is an unproductive complex.

ECorL-Neolactohexaose Complexes—The dominating conformation during a 100 ps dynamics simulation in vacuum of the complex between the branched oligosaccharide and ECorL, in which the β3-linked branch of conformer 6 was docked into the primary galactose binding site (designated ECorL-1), was extracted after 65 ps (see Fig. 4 and below). The initial dihedral angles for both Galβ4GlcNAc disaccharide segments were the same as those affording maximal interactions between GlcNAcβ3 and Gln219 (*6*, *9*). Initially the β6-linked branch was somewhat removed from the protein surface, but stable contacts were quickly established with the terminal Galβ4. Several additional interactions, which may explain the enhanced affinity of this ligand relative to neolactotetraosylceramide, are evident. The Tyr108 side chain is thus able to form hydrogen bonds with the 6-OH of the terminal Galβ4 and/or the 3-OH of the penultimate GlcNAcβ6. The backbone NH of Ser115 is also frequently within hydrogen bonding distance of Galβ4 6-OH. Furthermore, the nonpolar side of Galβ4 makes hydrophobic contact with the indole moiety of Trp135. As for the β3-linked branch, the same interactions as described above were seen throughout the entire simulation period. A water shell was subsequently added to the extracted conformer in order to explore possible stabilizing solvent-mediated interactions. During a 100 ps dynamics run an enhanced role of the water molecule interacting with Asn133 and the terminal Gal 2-OH (Table II), seen in the crystal structure of the lactose complex (*5*, *6*), was observed. Apart from the two interacting groups already mentioned, the Tyr108 hydroxyl, the GlcNAc 3-OH of the β6-linked branch, and the GlcNAc 6-OH of the β3-linked branch are also potential hydrogen bond partners, as shown in Fig. 4. However, the presence of a water molecule corresponding to the one bridging the Gly107 NH and Gal 3-OH groups, as found in the most recent lactose complex (*6*), is disallowed due to a slight reorientation of the Tyr108 side chain in the neolactohexaose complex. A number of other less tightly associated waters around the β3-linked branch, corresponding to those found in the lactose complex, were also seen (not shown).

As mentioned above, the β6-linked branch of conformer 6 may also be docked into the primary galactose binding site of ECorL (designated ECorL-2) without steric hindrance from the β3-linked branch. In the energy minimized structure, used as a starting structure for the subsequent dynamics run, the nonpolar side of the terminal Galβ4 of the β3-linked branch makes hydrophobic contact with the ring of Pro134. However, early into a 100 ps dynamics run, this branch moves towards Phe131, with the nonpolar side of Galβ4 eventually stacking up against the side chain of this residue, but from the opposite side of the β6-linked branch (not shown). Further hydrophobic interactions are found between the hydroxymethyl group of Galβ4 (β3-linked branch) and Pro134 and between the hydroxymethyl groups of both GlcNAc residues and the Phe131 ring. The β6-linked branch in the primary site displays the same

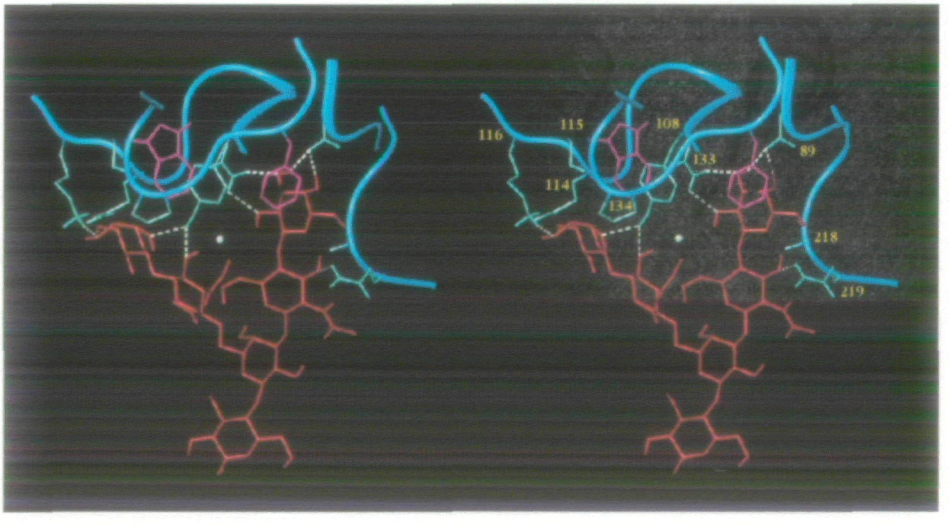

Fig. 4. **Stereo view of the complex between the oligosaccharide part of branched neolactohexaosylceramide [Galβ4GlcNAcβ6(Galβ4GlcNAcβ3)Galβ4Glcβ1Cer] and the lectin from *Erythrina corallodendron* (ECorL).** The dominating conformation of the complex in which the β3-linked branch occupies the primary galactose binding site was extracted 65 ps into a 100 ps molecular dynamics run at 300 K (ε = 6r) and subsequently energy minimized. Water was added to this conformer for an additional dynamics run of 100 ps (ε = 1) in order to locate favorable water interactions. The view shown here was extracted 34 ps into the simulation and energy minimized (ECorL-1 in Table III). The oligosaccharide is shown in red, the protein backbone in blue, and selected amino acid side chains in light blue, except for Phe131 and Trp135 (not labeled) which are purple. A bridging water molecule is shown as a small white sphere. The identity of the numbered amino acids are Asp89, Tyr108, Gln114, Ser115, Lys116, Asn133, Pro134, Ala218, and Gln219.

TABLE III. **Glycosidic dihedral angles for isolated branched neolactohexaose and in complex with ECorL or pIT.**

Disaccharide constituent	Glycosidic dihedral angles* (degrees)				
	Isolated (conformer 6)	ECorL-1 (water)	ECorL-2 (vacuum)	pLT	pLT (water)
Galβ4Glc	62/–6	57/–11	37/–60	61/–8	89/–12
GlcNAcβ3Gal	42/–60	36/–74	68/–22	35/–55	40/–45
Galβ4GlcNAcβ3	45/–33	55/–30	65/–5	25/–29	37/–28
GlcNAcβ6Gal	46/147/173	57/157/–175	51/122/137	94/176/180	160/138/89
Galβ4GlcNAcβ6	54/–15	30/–41	60/24	75/–10	70/46

*Glycosidic dihedral angles are defined in the legend to Fig. 1. Values for the oligosaccharide in the different complexes were obtained from energy minimized extracted conformers of the dynamics simulations described in the text.

interactions as mentioned earlier except for the side chain of Gln219, which in this case forms hydrogen bonds to the 6-OH groups of the GlcNAc residue on the β3-linked branch and the terminal Galβ4 on the β6-linked branch.

Glycosidic dihedral angles of the oligosaccharide in the complex where the β3-linked branch is in the primary site are not far removed from those found for the isolated oligosaccharide (ECorL-1 in Table III), suggesting a rather low energetic price in the formation of this complex. However, docking the β6-linked branch into the primary site results in significant changes in the dihedral angles of both branches due to movement of the terminal Galβ4 of the β3-linked branch towards Phe131. For both complexes, only marginal perturbations of the protein structure were observed. The average potential energy during the vacuum dynamics runs of the two complexes was approximately 7 kcal/mol in favor of ECorL-2, whereas the reverse was true for extracted energy minimized conformers. Since it is rather difficult to ascertain the relative importance of entropic factors for these complexes, it cannot be determined from these data alone which complex is the more populated one.

Binding of ECorL Mutants—One way of resolving this ambiguity is the use of genetically engineered forms of ECorL. The recombinant protein (rECorL) carries seven different amino acid substitutions of which only one is found in proximity to the binding site, namely Pro134Gln (*24*). For the ligands examined so far, no significant effects on the affinity of rECorL relative to ECorL have been discerned (*9*, *23*, *35*) since Gln134 borders the extended binding pocket into which *e.g.* fucosyl-*N*-acetyllactosamine binds. However, it is evident from Fig. 4 that the penultimate GlcNAc of the β6-linked branch is fairly close to Pro134 (~4 Å) and simple manipulation of the torsion angles of a glutamine side chain at this position reveals that in some instances steric interference with the β6-linked branch would occur, whereas for the ECorL-2 complex the β3-linked branch would be unobstructed by the Gln134 side chain. These inferences are corroborated by the results shown in Fig. 5A in which the affinity of rECorL for branched neolactohexaosylceramide is found to be considerably lower than for neolactotetraosylceramide.

Further substantiation comes from the binding of the Trp135Tyr mutant, which also carries the Pro134Gln mutation, to the same receptor structures. The Tyr135 side chain occupies the same space as the five-membered ring of the Trp135 indole moiety in the native protein (*35*). The combined effects of these two mutations completely abolishes binding of branched neolactohexaosylceramide and considerably reduces the binding of neolactotetraosylceramide (Fig. 5B, note the difference in vertical scale). These results stem from two effects: first, the terminal galactose of the β6-linked branch is denied hydrophobic interactions with the Tyr135 phenol moiety and, second, the Asn133 amide is most likely reorientated so that the -NH_2 group points toward the phenol hydroxyl whereby the hydrogen bonds to the terminal galactose of the β3-linked branch are weakened or lost. Only the second effect has any bearing on the neolactotetraosylceramide complex, hence the observed residual binding despite the fact that this compound shows the lower affinity of the two where native ECorL is concerned. Other ligands such as Fucα2Galβ4Glcβ and GalNAcβ are affected similarly (*35*). It is thus clear that the

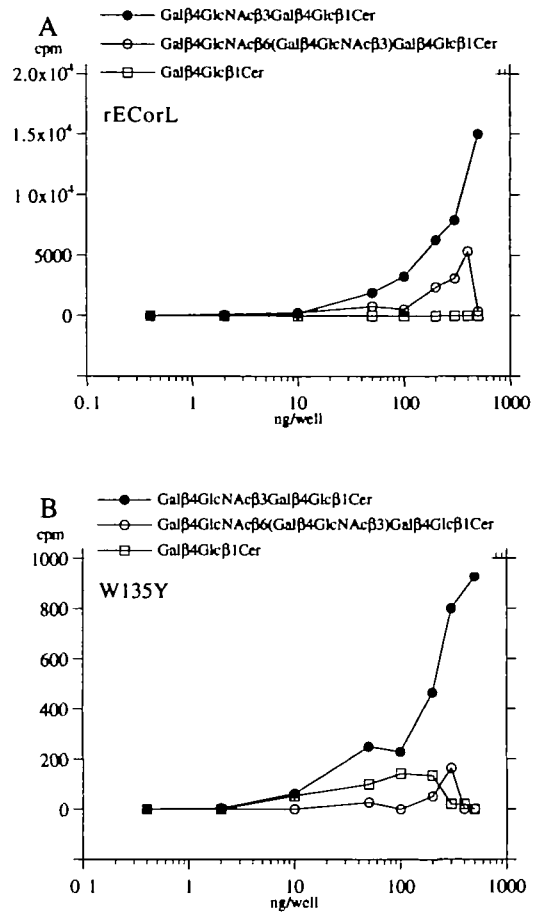

Fig. 5. **Microtiter well assay for the binding of recombinant *Erythrina corallodendron* lectin (rECorL) (A) and mutant Trp135Tyr (B) to *N*-acetyllactosamine-containing glycosphingolipids.** The proteins were ^{125}I-labeled and added to serial dilutions of glycosphingolipids adsorbed in microtiter wells. The data represent mean values of triplicate determinations.

ECorL-1 complex shown in Fig. 4 must be the one responsible for the observed binding of this compound, and that the alternative complex either is a low-affinity one, not picked up by the assay used here, or non-existent. Finally, inspection of the ECorL-1 complex reveals that extensions of the terminal Galβ4 of the β6-linked branch in either the 2-, 3-, 4-, or 6-position, by *e.g.* Fucα2, NeuAcα3/6 or Galβ4GlcNAcβ3, most likely would not be tolerated by the lectin.

pLT-Neolactohexaose Complex—Initial dynamics runs in vacuum on the pLT-neolactohexaose complex under a variety of conditions all led to unrealistic interactions. The terminal Galβ4 of the β3-linked branch of conformer 6, which was docked into the primary site, usually experienced upward (and sometimes twisting) movements of 2–4 Å, and the oligosaccharide as a whole folded in under the protein with the GlcNAcβ3Gal segment partially taking up the space occupied by sialic acid in the GM1 complex. Such arrangements would not allow realistic Glcβ1Cer linkage conformations to be assumed. However, crystal structures of various pLT complexes show that internal water molecules play a crucial role in stabilizing the different complexes (*7*, *36*). A series of 100 ps dynamics runs including decreasing amounts of explicit water molecules was there-

fore undertaken mainly in order to ascertain the limit of the stable interactions between the terminal Galβ4 and surrounding residues in the primary site. In the end it was found that as few as four water molecules on the inside of the binding cavity (see Fig. 6 for an overall view) were enough for a stable arrangement, even though the chosen dielectric constant ($\varepsilon = 1$) did not reflect the actual environment in the last dynamics runs. The subsequent dynamics run (250 ps), however, was performed in vacuum ($\varepsilon = 6r$) with these water molecules harmonically constrained around the oxygen atom positions (10 kcal/mol), since they were found at approximately the same positions, two of which correspond to the strongly bridging waters found in the lactose complex (Table II), regardless of the amount of water present. It was found necessary to introduce two further constraints as a consequence of the absence of a regular water shell: first, the positions of the C_α atoms of Ser55 and Gln56 were harmonically constrained (10 kcal/mol) to ensure the integrity of the primary site; second, the dihedral angles of the Galβ4Glc glycosidic linkage were restrained to values (Φ, Ψ = 62°, –6°) consistent with the presence of a ceramide linked to glucose in an extended conformation. The purpose of this dynamics run was mainly to allow the β6-linked branch to explore the conformational space available to it on a reasonable time scale.

A representative frame from the 250 ps dynamics run described above was extracted, after which explicit water was added for an additional 100 ps dynamics run without any constraints in order to locate further water interactions. A snapshot 34 ps into this latter run is shown in Fig. 6 and the glycosidic dihedral angles of the oligosaccharide are given in Table III. The dihedral angles are close to those of the isolated oligosaccharide except for the two linkages of the Galβ4GlcNAcβ6Gal segment, which deviate due to interactions with the protein. It is noteworthy that the Φ and ω angles of the GlcNAcβ6Gal linkage have undergone compensatory changes leaving the β6-linked branch in an orientation very similar to the one found in the vacuum simulation. However, on three brief occasions in the vacuum run, transitions to the angles found in water were observed. The galactose in the primary site displays its usual interactions with surrounding protein moieties whereas the terminal galactose of the β6-linked branch mainly interacts with the protein *via* its 6-OH group. In addition, an interresidue hydrogen bond between the hydroxymethyl groups of the two terminal galactoses was frequently observed. The penultimate GlcNAcβ3 of the β3-linked branch also showed stable interactions with the protein due to the acetamido moiety being lodged mainly between the Ile58 side chain and Gly33. Infrequently this moiety was found in front of the Ile58 side chain in the view shown in Fig. 6 as in the previous investigation of the pLT-neolactotetraose complex (*4*). However, performing a dynamics run on the pLT-neolactotetraose complex using the same conditions as for the branched compound, it was found that in this case as well, the acetamido moiety alternates between these two positions. Concerning the β6-linked branch, its interactions are mainly with the guanidino moiety of the Arg13 side chain, which most frequently establishes hydrogen bond interactions with the 6-O, but sometimes also with the 5-O of the terminal Gal (Fig. 6). The guanidino moiety displays further hydrogen bond interactions with the 2-O of the galactose at the branching point and occasionally with the 6-O of the GlcNAcβ3 residue. Water molecules contributing to the stability of the complex are shown as small white spheres in Fig. 6 and, apart from the four waters mentioned above, a fifth water molecule is found bridging the Arg13 side chain and the Glc 2-OH. The configuration of the pLT-neolactohexaose complex described above is consistent with the fact that pLT, in contrast to ECorL, tolerates extensions of the β6-linked branch (*10*) at either the 2-, 3-, or 4-position, even though it would lead to a minor reorientation of the terminal galactose.

Comparative Binding of Different B-Pentamers—The results related above point to Arg13 in pLT playing a major role in explaining the enhanced affinity for branched neolactohexaosylceramide. Confirmation of this observation was obtained by comparing the pLT binding of this compound to LT derived from a human strain of *E. coli* (hLT) as well as CT. The human LTB variant used here differs from pLTB at only four positions in its amino acid sequence, among them the crucial residue at position 13, which in the former protein is a histidine instead of an arginine (*37*, *38*). The three other substitutions are far removed from the binding site and are thus not expected to play any significant roles in this context. It is worth noting, however, that hLT from another human isolate also carries arginine at position 13 (*39*). Concerning CTB, approximately 80% homology with the LT toxins is observed, and also in this case, a histidine is found at position 13 (*40*). The results of the binding of these three variants to GM1, branched and linear neolactohexaosylceramides using the microtiter well assay are shown in Fig. 7. In order to be able to compare data for the latter two compounds, the amplitudes were normalized using the GM1 curves as standards since the saturation plateau is reached for this receptor. It is evident in all three cases that pLT binds much better than the other two toxins. For GM1, a substantial contribution to the higher affinity for pLT must be afforded by the presence of Arg13, since both hLT and CT bind with roughly the same strength. Also included in Fig. 7 are competition experiments (panel D) showing that hLT binding to neolactotetraosylceramide can be partially inhibited by preincubation with 10 mM neolactotetraose and completely blocked by 10 mM of GM1 pentasaccharide, indicating that neolactotetraosylceramide binds to the same site as GM1 and that the same conclusion can be inferred for branched neolactohexaosylceramide.

During a 250 ps dynamics run on the pLT-GM1 complex, the Arg13 side chain was found to interact strongly with the GalNAcβ4(NeuAcα3)Gal segment of GM1. The guanidino moiety is thus usually seen to hydrogen bond to the outermost carboxylate oxygen of sialic acid, the glycosidic oxygen of the NeuAcα3Gal linkage and the 2-O of the internal galactose (Fig. 8). Hydrogen bonds to the glycosidic oxygen of the GalNAcβ4Gal linkage and the carbonyl oxygen of the GalNAc acetamido moiety are also rather frequently observed. These observations differ from the interactions between Arg13 and GM1 suggested on the basis of the CT-GM1 complex (*34*), since here care was taken to avoid unlikely Galβ4Glc conformations in the absence of a ceramide by restraining the Φ and Ψ dihedral angles of this linkage (62°, –6°). In addition, a considerable entropic factor should contribute to the observed enhancement of the affinity. Other interactions, involving the terminal galactose and

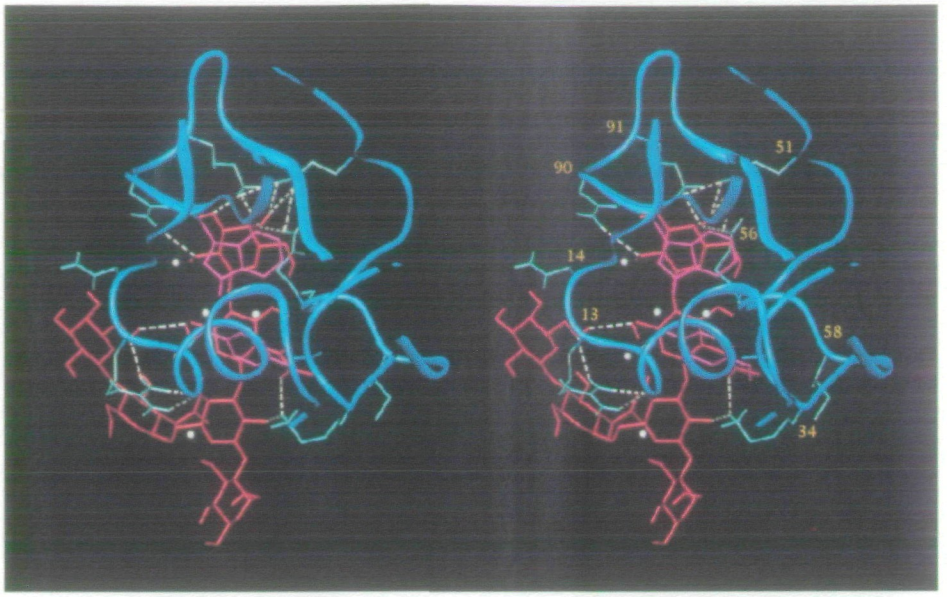

Fig. 6. **Stereo view of the complex between the oligosaccharide part of branched neolactohexaosylceramide [Galβ4GlcNAcβ6(Galβ4GlcNAcβ3)Galβ4Glcβ1Cer] and the heat-labile enterotoxin from *Escherichia coli* (pLT).** The dominating conformation of the complex in which the β3-linked branch occupies the primary galactose binding site was extracted 167 ps into a 250 ps molecular dynamics run at 300 K ($\varepsilon = 6r$) and subsequently energy minimized. Water was added to this conformer for an additional dynamics run of 100 ps ($\varepsilon = 1$) in order to locate favorable water interactions. The view shown here was extracted 34 ps into the simulation and energy minimized. The oligosaccharide is shown in red, the protein backbone in blue, and selected amino acid side chains in light blue, except for Tyr12 and Trp88, which are purple (not labeled). The $C_\alpha H_2$ of Gly33 is shown as blue sticks and bridging water molecules are shown as small white spheres. The identity of the numbered amino acids are Arg13, Asn14, Lys34, Glu51, Gln56, Ile58, Asn90, and Lys91.

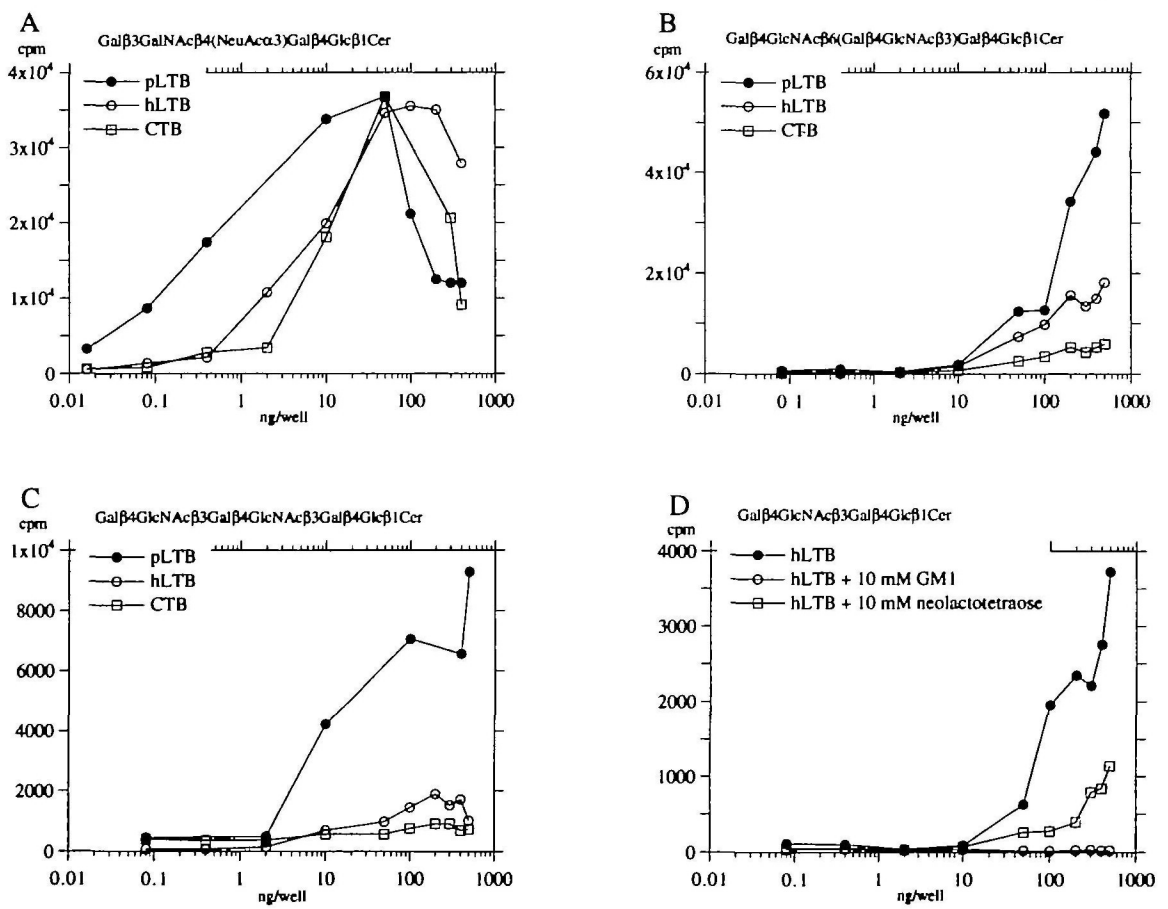

Fig. 7. **Microtiter well assay for the binding of porcine and human heat-labile toxin B-subunits (pLTB and hLTB, respectively) from *Escherichia coli* and cholera toxin B-subunits (CTB) to (A) GM1, (B) branched neolactohexaosylceramide and (C) linear neolactohexaosylceramide.** The effect of preincubation with GM1 pentasaccharide and neolactotetraose on the binding of hLTB to neolactotetraosylceramide is shown in (D). The proteins were ^{125}I-labeled and added to serial dilutions of glycosphingolipids adsorbed in microtiter wells. Incubation with saccharides was done as described under "MATERIALS AND METHODS." The data represent mean values of triplicate determinations. Data were normalized using the plateau values of the GM1 curves as standards except for panel D.

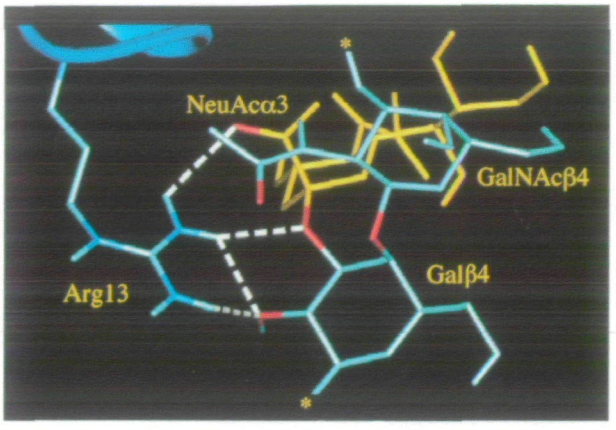

Fig. 8. **Close-up view of the complex between the oligosaccharide of GM1 [Galβ3GalNAcβ4(NeuAcα3)Galβ4Glcβ1Cer] and the heat-labile toxin from *Escherichia coli* (pLT) showing the affinity-enhancing role of Arg13.** One of several favorable conformations of the complex was extracted 186 ps into a 250 ps molecular dynamics run at 300 K (ε = 6r). The oligosaccharides are shown in light blue, except for sialic acid, which is yellow. The protein backbone is shown in blue and selected amino acid side chains in light blue. Oxygens to which the guanidino moiety of Arg13 forms hydrogen bonds during the dynamics simulation are indicated in red. The asterisks indicate where the terminal galactose and internal glucose are attached.

sialic acid were identical to those observed for the CT-GM1 complex (*34*).

Linear neolactohexaosylceramide behaves, as expected, similarly to neolactotetraosylceramide (*33*) in that a considerable drop in affinity occurs on going from pLT to hLT, again ascribable to the absence of arginine at position 13, whereas CT is non-binding (Fig. 7C). For branched neolactohexaosylceramide a similar but not as dramatic drop in affinity occurs when exchanging Arg for His at position 13, and even CT displays measurable binding (Fig. 7B). The slightly enhanced affinities of hLT and CT for the branched compound relative to the linear one can mainly be ascribed to van der Waals interactions between the $-C_\beta H_2$ group of His13 and the terminal galactose of the β6-linked branch and between Asn14 and 3-OH of the terminal galactose. Furthermore, the imidazole ring points away from the binding site and consequently does not participate in any interactions with any of the three ligands.

Concluding Remarks—Of the several three-dimensional structures of lectins in complex with branched oligosaccharides that are available, the majority involve sugars having a trimannoside core, with the notable exception of soybean agglutinin in complex with different biantennary blood group I analogs (*41*). However, these latter complexes, including the one containing the analog in which the *N*-acetyllactosamine branches are β3- and β6-linked, were obtained under conditions favoring cross-linked lattices. Concerning the LT and CT toxins, no structural information regarding the binding of branched *N*-acetyllactosamine–based compounds is available. Theoretical studies are also limited, and deal mainly with the conformational characteristics of isolated oligosaccharides and their compatibility with known crystal structures or homologous ones (*29*, *42*). The approach adopted in the present study utilizes the known binding mode in the primary binding site of both ECorL and LT for docking reasonable starting geometries of branched neolactohexaose into the respective proteins, and subsequently letting the dynamics of the system be the decisive factor for establishing the additional interactions that must be present in order to explain the enhanced binding affinities relative to linear *N*-acetyllactosamine–containing structures. The picture arrived at for either complex is compatible with (a) the relative affinities of the proteins for the different glycosphingolipids that were tested; (b) effects of mutations in the binding site region, either engineered or naturally occurring ones; and (c) tolerance or non-tolerance of extensions on the β6-linked branch. Despite these findings, there are some limitations in the present study. For example, it cannot totally be excluded that the systems during the dynamics runs were trapped in local energy minima other than the ones representing the true conformations. Furthermore, water interactions, at present computationally impossible to include from the outset, were introduced after the protein–carbohydrate interactions had been established, which might influence the outcome of the simulations. However, a number of the bridging water molecules, as well as other less tightly associated waters, seen in the crystal complexes were also found in this study, suggesting that this approach is valid at least for the two systems investigated here.

We are indepted to Professor Nathan Sharon and Dr. Rivka Adar for supplying us with rECorL and the Trp135Tyr mutant, and Professor Timothy Hirst for providing pLTB and hLTB.

REFERENCES

1. Sharon, N. and Lis, H. (1989) Carbohydrate specificity in *Lectins*, pp. 37–46, Chapman and Hall, London
2. Spangler, B.D. (1992) Structure and function of cholera toxin and the related *Escherichia coli* heat-labile enterotoxin. *Microbiol. Rev.* **56**, 622–647
3. Teneberg, S., Ångström, J., Jovall, P.-Å., and Karlsson, K.-A. (1994) Characterization of binding of Galβ4GlcNAc-specific lectins from *Erythrina cristagalli* and *Erythrina corallodendron* to glycosphingolipids. Detection, isolation and characterization of a novel glycosphingolipid of bovine buttermilk. *J. Biol. Chem.* **269**, 8554–8563
4. Teneberg, S., Hirst, T.R., Ångström, J., and Karlsson, K.-A. (1994) Comparison of glycolipid-binding specificities of cholera toxin and porcine *Escherichia coli* heat-labile enterotoxin: identification of a receptor-active non-ganglioside glycolipid for the heat-labile toxin in infant rabbit small intestine. *Glycoconj. J.* **11**, 533–540
5. Shaanan, B., Lis, H., and Sharon, N. (1991) Structure of a legume lectin with an ordered *N*-linked carbohydrate in complex with lactose. *Science* **254**, 862–866
6. Elgavish, S. and Shaanan, B. (1998) Structures of the *Erythrina corallodendron* lectin and of its complexes with mono- and disaccharides. *J. Mol. Biol.* **277**, 917–932
7. Sixma, T.K., Pronk, S.E., Kalk, K.H., van Zanten, B.A.M., Berghuis, A.M., and Hol, W.G.J. (1992) Lactose binding to heat-labile enterotoxin revealed by X-ray crystallography. *Nature* **355**, 561–564
8. Merritt, E.A., Sixma, T.K., Kalk, K.H., van Zanten, B.A.M., and Hol, W.G.J. (1994) Galactose-binding site in *Escherichia coli* heat-labile enterotoxin (LT) and cholera toxin (CT). *Mol. Microbiol.* **13**, 745–753
9. Moreno, E., Teneberg, S., Adar, R., Sharon, N., Karlsson, K.-A., and Ångström, J. (1997) Redefinition of the carbohydrate specificity of *Erythrina corallodendron* lectin based on solid-phase binding assays and molecular modeling of native and recombinant forms obtained by site-directed mutagenesis. *Biochemistry*

36, 4429–4437
10. Karlsson, K.-A., Teneberg, S., Ångström, J., Kjellberg, A., Hirst, T.R., Bergström, J., and Miller-Podraza, H. (1996) Unexpected carbohydrate cross-binding by *Escherichia coli* heat-labile enterotoxin. Recognition of human and rabbit target cell glycoconjugates in comparison with cholera toxin. *Bioorg. Med. Chem.* **4**, 1919–1928
11. Holmgren, J., Fredman, P., Lindblad, M., Svennerholm, A.M., and Svennerholm, L. (1982) Rabbit intestinal glycoprotein receptor for *Escherichia coli* heat-labile enterotoxin lacking affinity for cholera toxin. *Infect. Immun.* **38**, 424–433
12. Holmgren, J., Lindblad, M., Fredman, P., Svennerholm, L., and Myrvold, H. (1985) Comparison of receptors for cholera and *Escherichia coli* enterotoxins in human intestine. *Gastroenterology* **89**, 27–35
13. Holmgren, J. (1994) Receptors for cholera toxin and *Escherichia coli* heat-labile enterotoxin revisited in *Progress in Brain Research* (Svennerholm, L., Asbury, A.K., Reisfeld, R.A., Sandhoff, K., Suzuki, K., Tettamanti, G., and Toffano, G., eds.) Vol. 101, pp. 163–177, Elsevier Science BV
14. Orlandi, P.A., Critchley, D.R., and Fishman, P.H. (1994) The heat-labile enterotoxin of *Escherichia coli* binds to polylactosaminoglycan-containing receptors in CaCo-2 human intestinal epithelial cells. *Biochemistry* **33**, 12886–12895
15. Griffiths, S.L. and Critchley, D.R. (1991) Characterization of the binding sites for *Escherichia coli* heat-labile toxin type I in intestinal brush borders. *Biochim. Biophys. Acta* **1075**, 154–161
16. Shida, K., Takamizawa, K., Takeda, T., and Osawa, T. (1996) Characterization by Western blotting of mouse intestinal glycoproteins bound by *Escherichia coli* heat-labile enterotoxin type I. *Microbiol. Immunol.* **40**, 71–75
17. Rini, J.M. (1995) Lectin structure. *Annu. Rev. Biophys. Biomol. Struct.* **24**, 551–577
18. Karlsson, K.-A. (1987) Preparation of total non-acid glycolipids for overlay analysis of receptors for bacteria and viruses and for other studies. *Methods Enzymol.* **138**, 212–220
19. Hansson, G.C., Karlsson, K.-A., Larson, G., McKibbin, J.M., Strömberg, N., and Thurin, J. (1983) Isoglobotriaosylceramide and the Forssman glycolipid of dog small intestine occupy separate tissue compartments and differ in ceramide structure. *Biochim. Biophys. Acta* **750**, 214–216
20. Laine, R.A., Stellner, K., and Hakomori, S.-i. (1974) Isolation and characterization of membrane glycosphingolipids. *Methods Membr. Biol.* **2**, 205–244
21. Hakomori, S.-i. (1983) Chemistry of glycosphingolipids in *Sphingolipid Biochemistry* (Hanfer, J.N. and Hakomori, S.-i., eds.) Vol. 3, pp. 1–165, Plenum Press, New York
22. Iwamori, M. and Nagai, Y. (1981) Ganglioside composition of rabbit thymus. *Biochim. Biohpys. Acta* **665**, 205–213
23. Adar, R. and Sharon, N. (1996) Mutational studies of the amino acids in the combining site of *Erythrina corallodendron* lectin. *Eur. J. Biochem.* **239**, 668–674
24. Arango, R., Rozenblatt, S., and Sharon, N. (1990) Cloning and sequence analysis of the *Erythrina corallodendron* lectin cDNA. *FEBS Lett.* **264**, 109–111
25. Amin, T. and Hirst, T. (1994) Purification of the B-subunit of *Escherichia coli* heat-labile enterotoxin by heterologous expression and secretion in a marine vibrio. *Protein Expr. Purif.* **5**, 198–204
26. Aggarwal, B.B., Eessalu, T.E., and Hass, P.E. (1985) Characterization of receptors for human tumour necrosis factor and their regulation by γ-interferon. *Nature* **318**, 665–667
27. Karlsson, K.-A. and Strömberg, N. (1987) Overlay and solid-phase analysis of glycolipid receptors for bacteria. *Methods Enzymol.* **138**, 220–232
28. Bourne, Y., Rougé, P., and Cambillau, C. (1992) X-ray structure of a biantennary octasaccharide-lectin complex refined at 2.3-Å resolution. *J. Biol. Chem.* **267**, 197–203
29. Imberty, A., Delage, M.-M., Bourne, Y., Cambillau, C., and Pérez, S. (1991) Data bank of three-dimensional structures of disaccharides: Part II. *N*-Acetyllactosaminic type *N*-glycans. Comparison with the crystal structure of a biantennary octasaccharide. *Glycoconj. J.* **8**, 456–483
30. Bock, K., Breimer, M.E., Brignole, A., Hansson, G.C., Karlsson, K.-A., Larson, G., Leffler, H., Samuelsson, B.E., Strömberg, N., Svanborg-Edén, C., and Thurin, J. (1985) Specificity of binding of a strain of uropathogenic *Escherichia coli* to Galα1→4Gal-containing glycosphingolipids. *J. Biol. Chem.* **260**, 8545–8551
31. Bourne, Y., Rougé, P., and Cambillau, C. (1990) X-ray structure of a (α-Man(1-3)β-Man(1-4)GlcNAc)-lectin complex at 2.1-Å resolution. The role of water in sugar-lectin interaction. *J. Biol. Chem.* **265**, 18161–18165
32. Çagin, T, Goddard III, W.A., and Ary, M.L. (1991) Canonical dynamics simulations of single-chain polyethene. *Comput. Polym. Sci.* **1**, 241–248
33. Bäckström, M., Shahabi, V., Johansson, S., Teneberg, S., Kjellberg, A., Miller-Podraza, H., Holmgren, J., and Lebens, M. (1997) Structural basis for differential receptor binding of cholera and *Escherichia coli* heat-labile toxins: influence of heterologous amino acid substitutions in the cholera B-subunit. *Mol. Microbiol.* **24**, 489–497
34. Merritt, E.A., Sarfaty, S., van den Akker, F., L'hoir, C., Martial, J.A., and Hol, W.G.J. (1994) Crystal structure of cholera toxin B-pentamer bound to receptor G_{M1} pentasaccharide. *Protein Sci.* **3**, 166–175
35. Adar, R., Moreno, E., Streicher, H., Karlsson, K.-A., Ångström, J., and Sharon, N. (1998) Structural features of the combining site region of *Erythrina corallodendron* lectin: Role of tryptophan 135. *Protein Sci.* **7**, 52–63
36. Merritt, E.A., Sarfaty, S., Feil, I.K., and Hol, W.G.J. (1997) Structural foundation for the design of receptor antagonists targeting *Escherichia coli* heat-labile enterotoxin. *Structure* **5**, 1485–1499
37. Dallas, W.S. (1983) Conformity between heat-labile toxin genes from human and porcine enterotoxigenic *Escherichia coli*. *Infect. Immun.* **40**, 647–652
38. Leong, J., Vinal, A.C., and Dallas, W.S. (1985) Nucleotide sequence comparison between heat-labile toxin B-subunit cistrons from *Escherichia coli* of human and porcine origin. *Infect. Immun.* **48**, 73–77
39. Tsuji, T., Iida, T., Honda, T., Miwatani, T., Nagahama, M., Sakurai, J., and Matsubara, H. (1987) A unique amino acid sequence of the B subunit of a heat-labile enterotoxin isolated from a human enterotoxigenic *Escherichia coli*. *Microb. Pathol.* **2**, 381–390
40. Dallas, W.S. and Falkow, S. (1980) Amino acid sequence homology between cholera toxin and *Escherichia coli* heat-labile toxin. *Nature* **288**, 499–501
41. Olsen, L.R., Dessen, A., Gupta, D., Sabesan, S., Sacchettini, J.C., and Brewer, C.F. (1997) X-ray crystallographic studies of unique cross-linked lattices between four isomeric biantennary oligosaccharides and soybean agglutinin. *Biochemistry* **36**, 15073-15080
42. Sokolowski, T., Peters, T., Pérez, S., and Imberty, A. (1997) Conformational analysis of biantennary glycans and molecular modeling of their complexes with lentil lectin. *J. Mol. Graph. Model.* **15**, 37–42